Open Access

Advances in Environmental and Engineering Research

LIDSEN Publishing Inc.

Original Research

Variations in the Maximum Electron Density of the F_2 Layer (N_mF_2) over the Middle Latitude Station of Grahamstown, South Africa, during Solar Cycle 23

Aghogho Ogwala [1, 2, *], Eugene Onori [2], Cornelius Ogabi [2], Oluwafunmilayo Ometan [2], Yusuf Kayode [2], Rasaq Adewemimo Adeniji-Adele [2], Emmanuel Somoye [2], Janet Odewale [2]

1. Eko University of Medicine and Health Sciences, Ijanikin, Lagos, Nigeria; E-Mail: ogwala02@gmail.com
2. Lagos State University, Ojo, Lagos, Nigeria; E-Mails: onorieugene@gmail.com; drkunleogabi@gmail.com; ometanfunmi@gmail.com; kayodeyusuf1988@gmail.com; adelleradelle@gmail.com; emmanuel.somoye@lasu.edu.ng; jaymamajane@gmail.com

* **Correspondence:** Ogwala Aghogho; E-Mail: ogwala02@gmail.com

Academic Editor: Zed Rengel

Adv Environ Eng Res
2022, volume 3, issue 4
doi:10.21926/aeer.2204048

Received: September 13, 2022
Accepted: November 18, 2022
Published: December 05, 2022

Abstract

Ultraviolet (UV) and X-ray radiation are the primary causes of ionization that produce electron density in sufficient quantities to promote the propagation of satellite radio signals in the ionosphere. The electron densities suffer from spatio-temporal variations, and this poses different degrees of threats to satellite radio signals propagating through the ionosphere. We aimed to characterize the maximum electron density of the F_2 layer (N_mF_2) in the middle-latitude ionosphere over Grahamstown, South Africa (Geographic latitude: 33.30°S, Geographic longitude: 26.50°E; Geomagnetic Latitude: 33.92°S, Geomagnetic Longitude: 89.37°E). The mean N_mF_2 data for solar cycle 23 (1998–2008) were used for the studies. The data were grouped into the high solar activity (HSA: 2000–2002), moderate solar activity (MSA: 1998–1999, 2003–2005), and low solar activity (LSA: 2006–2008) years. N_mF_2 variations were characterized based on the diurnal, seasonal, monthly, and annual data. Also, the correlation between N_mF_2 and the sunspot number was investigated. Results on diurnal and seasonal variations revealed that noontime bite-out of N_mF_2 was observed during the June solstice every year. However, it was not observed in the other three seasons. Equinoctial asymmetry is observed to show insignificant annual and solar cycle variations. The seasonal and annual variations of N_mF_2 with sunspot number were linear (exception: June solstice for MSA, the year 1999; HSA, years 2000–2001). The results reveal that the correlation between N_mF_2 and the sunspot number was insignificant under conditions of the annual, solar cycle, and latitudinal variations (exception: MSA, the year 2005; negative correlation (0.64)).

Keywords
N_mF_2 variations; noon bite-out; southern middle latitude; seasonal; solar activity; correlation coefficient

1. Introduction

The ionosphere is formed at altitudes between 60–1000 km, where the X-rays and ultraviolet (UV) radiations from the Sun collide with electrons and knock off electrons from the outermost shell of neutral particles. These electrons pose different degrees of threats to the ground and space-based technological systems such as satellite communication links, hardware, avionics, and navigation control devices [1]. The severity of these effects is observed in regions spanning from equatorial/low-latitude to high-latitudes. It has been observed that the degree of the effect exerted at equatorial/low- and high-latitude regions is higher than the degree of the effect exerted at middle-latitude regions. However, the middle-latitude ionospheric effects on modern technological systems cannot be overlooked because of their unpredictable and dynamic nature [2].

The middle-latitude ionosphere is the quietest region which undergoes the least variations in almost all sectors barring the African longitude. This may be attributed to the nearly horizontal orientation of the geomagnetic field lines running through the African sector. The middle latitude is also the best understood ionospheric region as the region has been widely explored using various ionospheric observation equipment such as ionosonde/digisonde, global positioning system (GPS) receivers, and incoherent scatter radar (ISR). Hence, transient variations in the middle latitude ionospheric region, including the main ionospheric trough (MIT), which is usually driven by solar and geomagnetic storms, have been reported [3]. Also, the interaction between the equator-ward disturbances in this region and the ionospheric plasma (and components of the neutral atmospheric wind) affects the movement of ions. The balance between the production and loss rates is also affected [4]. The extent of solar ionization realized in this region is depleted under conditions of chemical recombination. These disturbances affect the propagation of the satellite radio wave at middle latitudes. Seasonal and winter anomalies (majorly equatorial/low latitude ionospheric phenomena) have also been reported at the middle latitude F region. These anomalies have been primarily recorded during solar maximum [5]. Apart from the seasonal and winter anomalies, the middle-latitude ionospheric phenomena, in most cases, deviate completely from the equatorial/low and high-latitude ionospheric phenomena. For example, Somoye [6] reported insignificant differences between various ionospheric features such as pre- and post-noon peaks, morning depression, and the rate of fall of N_mF_2 in the evening over a solar cycle at a middle-latitude station of Slough. The f_oF_2/N_mF_2 data were analyzed to arrive at the results. Chen et al. [7] reported that the degree of equinoctial asymmetry of N_mF_2 increases as solar activity increases in the middle latitudes. The increase observed in these regions was higher than the increase observed in low-latitude regions. Aggarwal et al. [8] and Talha et al. [9] have described the ionospheric phenomenon responsible for equinoctial asymmetry in detail. Chen et al. [7] reported that the rate of increase in N_mF_2 with an increase in the Solar Radio Flux ($F_{10.7}$) is higher during the March equinox (compared to that observed during the September equinox) at middle latitudes. Talha et al. [9] reported that the equatorial anomaly (EA) was high at low/middle latitude regions due to the presence of extreme UV radiation (EUV).

The variations in f_oF_2/N_mF_2 across different latitudes and longitudes have been previously studied [5, 10-21]. The N_mF_2 variability under different geomagnetic conditions was studied with reference to the quite time ionospheric condition. The middle-latitude ionospheric region has been widely investigated in the past, but most of these studies focused on the Asian and American sectors. The middle-latitude ionosphere in Africa remains the least explored region. This can be attributed to the sparse distribution of ground-based ionospheric observation equipment in the African sector. However, the recent installation of Ionosonde/Digisonde by the South African National Space Agency (SANSA) in a few locations in the South African middle-latitude has helped obtain f_oF_2/N_mF_2 data for ionospheric research. Hence, more studies should be conducted to reinforce the past efforts of scientists to better understand the complex seasonal variations observed in the African middle-latitude ionosphere.

The composition of neutral wind, electric field, diffusion properties, and temperature variations significantly influence the middle latitude regions of the ionosphere. This observation is supported by the movement of plasma from the equator to high-latitude regions [22]. All these effects can result in transient variations in N_mF_2 and h_mF_2 [20, 23, 24]. Furthermore, like the equatorial/low latitude ionosphere, the middle latitude ionosphere also plays a crucial role in the propagation of distant satellite radio communication waves. Therefore, the aim of this research is to characterize the variations in the middle latitude N_mF_2 during solar cycle 23 (1998–2008) at Grahamstown, South Africa.

2. Data and Methodology

2.1 Data

Hourly data for the maximum electron density of the F_2 layer (N_mF_2) were used for the studies. The data were obtained by calculating the hourly values of the critical frequency of the F_2 layer (f_oF_2). The data were obtained from the ground-based digisonde at Grahamstown (Geographic latitude: 33.30°S, Geographic longitude: 26.50°E; Geomagnetic latitude: 33.92°S, Geomagnetic Longitude: 89.37°E), a middle latitude station located in South Africa. The hourly f_oF_2/N_mF_2 data were obtained from the Global Ionosphere Radio Observatory (GIRO) website (https://giro.uml.edu/didbase/) under the authorization of the South Africa National Space Agency (SANSA). Data corresponding to sunspot number (R_z) were obtained from the National Geophysical Data Center (NGDC: www.ngdc.noaa.gov/) website. Data were collected over 1998–2008, and the years were classified into Low Solar Activity (LSA) years, Moderate Solar Activity (MSA) years, and High Solar Activity (HSA) years (Table 1).

Table 1 Solar cycle epoch, years, and equivalent sunspot numbers (Rz).

Solar Cycle Epoch	Year	Sunspot Number
HSA	2000	120
HSA	2001	111
HSA	2002	104
MSA	1998	69
MSA	1999	93
MSA	2003	64
MSA	2004	40
MSA	2005	30
LSA	2006	15
LSA	2007	8
LSA	2008	3

The N_mF_2 values were calculated from the f_oF_2 values using equation 1 as follows:

$$N_mF_2 = \frac{(foF2)^2}{80.6}, \quad (1)$$

where f_oF_2 is presented in the units of MHz, and N_mF_2 is measured in the units of $\times 10^{12}$ electrons per cubic meter ($\times 10^{12}$ el/m^3).

When $R_z > 100$, the data are grouped under HSA, when $100 \geq R_z \geq 20$ the data are grouped under MSA, and when $R_z < 20$ the data are grouped under LSA [25]. Table 1 presents the solar cycle epoch, year, and the corresponding sunspot number (Rz).

2.2 Methodology

2.2.1 Diurnal and Seasonal Variations in N_mF_2

The statistical average was calculated based on the hourly mean of N_mF_2 to obtain the monthly mean values to investigate the diurnal variations in N_mF_2. For seasonal variations, the monthly mean values were further grouped into four seasons [26]: March equinox (February, March, and April), June solstice (May, June, and July), September equinox (August, September, and October) and December solstice (November, December, and January). The groups were constructed by taking the average data recorded over the three months that constituted each season. Furthermore, we estimated the percentage differences between the data obtained during the March equinox (ME) and that recorded during the September equinox (SE) using the method followed by Chen et al. [7], using equation (2) as follows:

$$\%\, difference = \left(\frac{ME - SE}{SE}\right) \times 100 \quad (2)$$

2.2.2 Seasonal and Annual Variations in N_mF_2 over a Solar Cycle

The seasonal and annual variations in the mean N_mF_2 values over a solar cycle were also analyzed and grouped into three solar cycle epochs (LSA, MSA, and HSA; Table 1).

2.2.3 Correlation Coefficient (r) describing the correlation between N_mF_2 and the Sunspot Number

The correlation between N_mF_2 and the sunspot number was statistically analyzed. The correlation coefficient is the measure of the strength of the linear relationship between two variables. It is given by equation (3) as follows:

$$r = \frac{n\sum xy - \sum x \sum y}{\sqrt{\{n\sum x^2 - (\sum x)^2\}\{n\sum y^2 - (\sum y)^2\}}}, \quad (3)$$

where 'x' and 'y' are independent variables that represent N_mF_2 and R_z, respectively, while 'n' is the number of each variable. We classified correlation coefficients using the process followed by Mukaka (2012)[27]. The groups were labeled very high correlation (r between ±0.90 and ±1.0), high correlation (r between ±0.70 and ±0.89), moderate correlation (r between ±0.50 and ±0.69), low correlation (r between ±0.30 and ±0.49), and negligible correlation (r between 0.0 and ±0.29).

3. Results and Discussions

3.1 Diurnal Variations in N_mF_2

Figure 1(a-k) shows the diurnal variations in N_mF_2 under conditions of different solar activities (HSA, MSA, and LSA). The data were recorded for solar cycle 23 at Grahamstown, South Africa. Similar diurnal variations were observed over the years for N_mF_2 for the three solar activity epochs. Analysis of the plots revealed the N_mF_2 values recorded during the day were higher than the values recorded during the night, and this could be attributed to the phenomenon of daytime solar ionization. During LSA ($R_z < 20$; 2006, 2007, 2008), diurnal variations in N_mF_2 increased. The minimum values were recorded during the early hours of the day between 02:00–03:00 UT, and the maximum values were recorded between 11:00–13:00 UT. The values reduced and reached the minimum values again at around sunset. During MSA ($100 \geq R_z \geq 20$; 1998, 1999, 2003–2005), the N_mF_2 value increased between 01:00 – 03:00 UT and reached the peak value gradually (09:00–13:00 UT), before reducing to the minimum value at sunset. During HSA ($R_z > 100$; 2000–2002), the N_mF_2 value started increasing from the minimum value (recorded at 02:00–03:00 UT) to the maximum value at 10:00–13:00 UT. Subsequently, the value decreased to the minimum value around sunset. When the figures were analyzed, an interesting observation was made for the middle-latitude N_mF_2 values. The nighttime enhancement in N_mF_2 was not observed, in contrast to the equatorial and low-latitude N_mF_2 values, which often show nighttime enhancement for the electron density profile. The absence of nighttime enhancement in N_mF_2 at the middle latitude region may be attributed to the weakening of the eastward electric field. This results in insignificant pre-reversal enhancement of the ionospheric zonal electric field toward higher latitudes during post-sunset hours, just before the electric field current reverses toward the west in the night [28, 29].

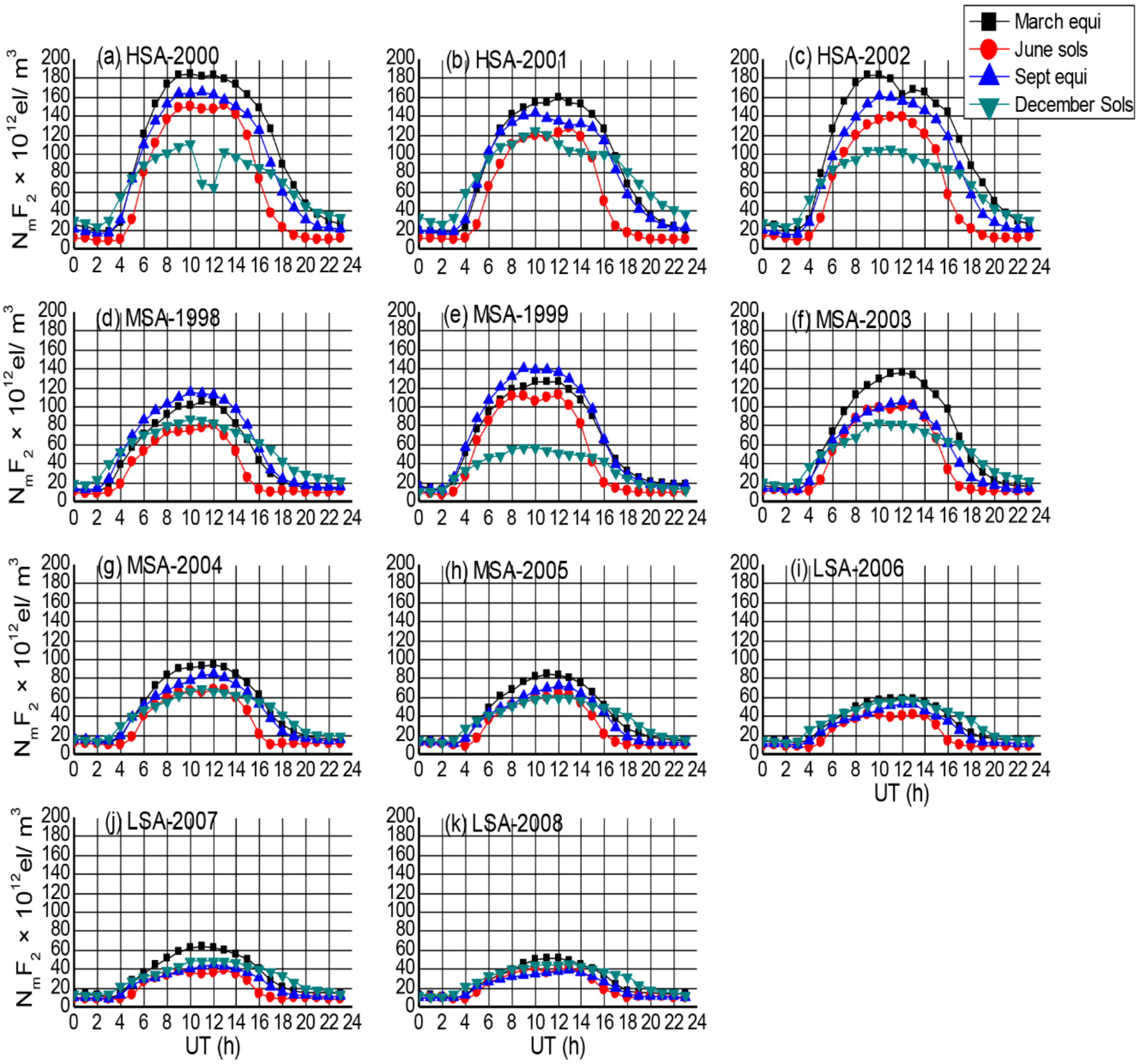

Figure 1 (a-k): Diurnal and seasonal variations in the mean N_mF_2 values recorded during the HSA years of 2000, 2001, and 2002, MSA years of 1998, 1999, 2003, 2004, and 2005, and LSA years of 2006, 2007, and 2008 (solar cycle 23 at Grahamstown, South Africa).

3.2 Seasonal Variations in N_mF_2

Figure 1(a–k) also shows the seasonal variations in N_mF_2 during the different solar activity epochs (HSA, MSA, and LSA). The data were collected for solar cycle 23 at Grahamstown, South Africa. Variations in the shapes of N_mF_2 are observed during the four seasons. However, these variations are quite insignificant for the three solar activity epochs. Typical features, such as the noontime bite-out phenomenon, are observed in some of the seasons (especially during June solstice) for the low-latitude regions. During LSA (Figure 1(i-k); 2006–2008), noontime bite-out is observed at 11:00 UT during June solstice. The magnitudes of the intensities of the pre-noon and post-noon peaks vary. Dome-shaped peaks are recorded midday (12:00 UT) during other seasons (during March and September equinoxes and December solstice). The N_mF_2 values recorded during the equinoxes are higher than those recorded during the solstices during the three LSA years. The trend deviated in the year 2006 when the values recorded from 06:00–15:00 UT during the March equinox and December solstice were comparable (36–58 × 10^{12} el/m^3). Comparable values were also recorded between 21:00–03:00 UT. Figure 2(a-k) presents equinoctial asymmetry, i.e., the statistical differences between the values recorded during the March equinox (ME) and September equinox (SE). Figure 2(i-k) presents equinoctial asymmetry. It was observed that the N_mF_2 values recorded during ME were higher than the values recorded during SE over the LSA years. The differences between the pre-midnight and post-midnight N_mF_2 values recorded over the four seasons of the LSA years were insignificant. Equatorial and low-latitude winter anomaly was observed during the LSA years. During the MSA years, noontime bite-out curves with varying magnitudes of pre- and post-noon peaks were observed during the June solstice, while the dome-shaped peaks were observed during equinoxes. However, broader peaks during all MSA years were observed during the December solstice. The N_mF_2 values recorded during equinoxes were higher than those recorded during the solstices (exception: MSA year of 2003) (Figure 1f). The daytime N_mF_2 values recorded during the September equinox and June solstice were comparable and in the same range between 07:00–14:00 UT (70–100 × 10^{12} el/m^3). Also, analysis of the daytime N_mF_2 value recorded for the MSA year of 2004 (Figure 1 g) reveals that the magnitudes recorded during December and June solstice were comparable between 07:00–14:00 UT (51–63 × 10^{12} el/m^3). The observed equinoctial asymmetry was obvious from all MSA plots (Figure 2). While SE magnitudes were higher than ME magnitudes during the MSA years (Figures 2(d-e)), the reverse was true for the MSA years (2003–2005) (Figures 2(f-h)). Furthermore, the differences between the pre-midnight and post-midnight N_mF_2 values were insignificant for all seasons of all MSA years. During most of the MSA years, a deviation from the equatorial/low-latitude winter anomaly was observed. This is in contrast to the observation made during the MSA year 1998 and LSA years spanning 2006–2008). The magnitude recorded in these years during the June solstice magnitude was observed to be higher than the magnitude recorded during the December solstice. This was particularly prominent for the MSA year (1999) when the differences in the magnitudes recorded during the June and December solstices were in the range of 50–60 × 10^{12} el/m^3. During the HSA years, a noon bite-out profile was observed during the June solstice. An exception was observed for the HSA year of 2002 (Figure 1c) when a dome-shaped peak was observed. The noon bite-out phenomenon with pre- and post-noon peaks of varying intensities was observed during the December solstice of the HSA years of 2000 – 2001 (Figure 1a-1b), March equinox of the HSA year of 2002 (Figure 1c), and September equinox of the HSA year of 2001 (Figure 1b). In all other seasons, either a dome-shaped peak or a peak shift from pre-noon to post-noon periods were observed for the HSA years. A broad daytime peak with a slight depression during post-noon periods (14:00–16:00 UT) was observed during the December solstice of the HSA year 2002 (Figure 1c). The N_mF_2 values recorded during the equinoxes were higher than those recorded during the solstices (Figures 1(a-c)). ME and SE of similar magnitudes were recorded during the first few hours of the day, after which the ME magnitude remained higher than the SE magnitudes for the remaining hours of the day in all the HSA years (Figures 2(a-c)). Pre-midnight peaks are slightly higher than post-midnight peaks in all HSA seasons. An exception was recorded during the June solstice when insignificant differences between the pre- and post-midnight peaks were observed. Deviations from the winter anomaly, which is peculiar to equatorial and low latitudes, were observed during the HSA years.

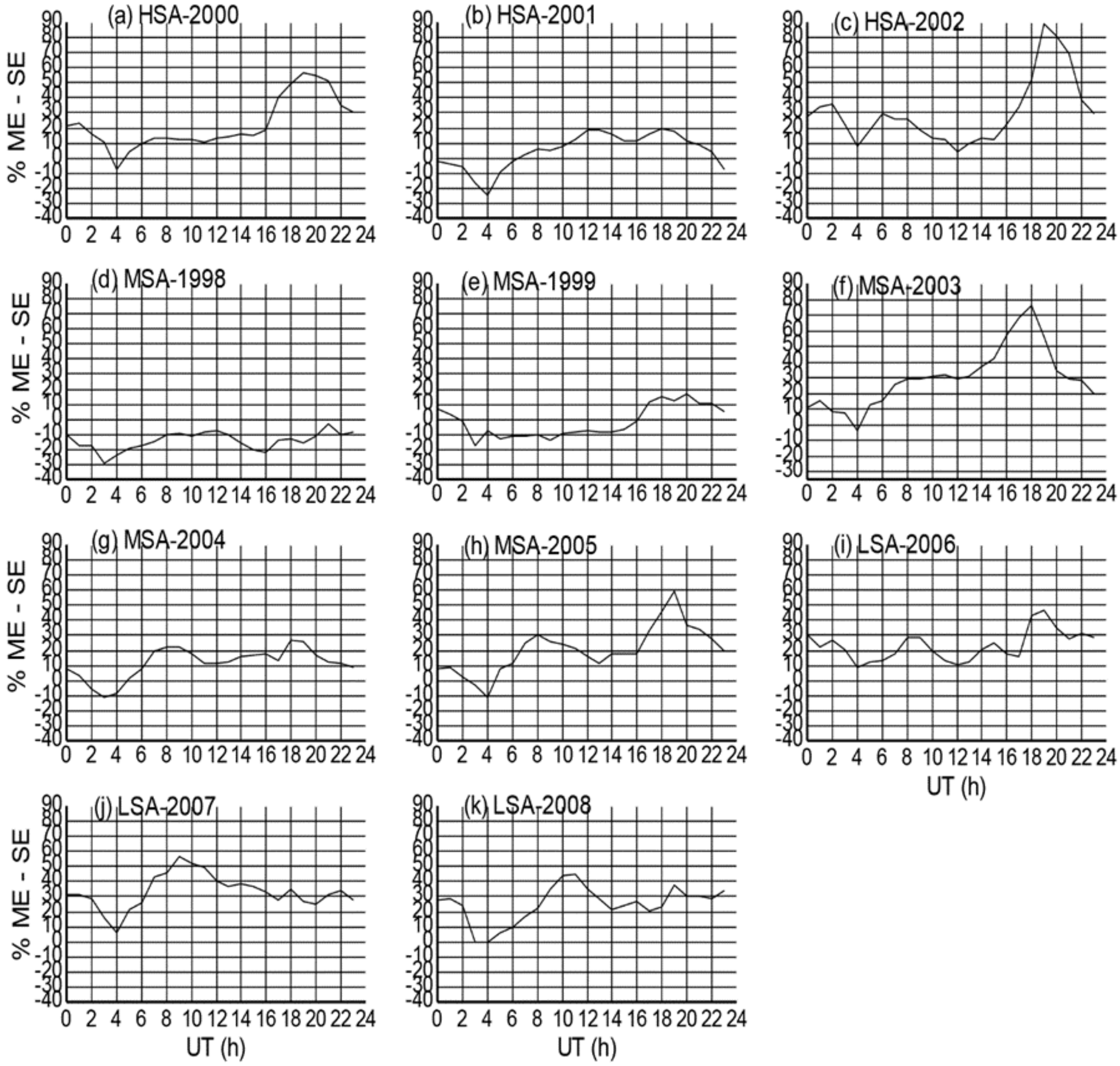

Figure 2 (a-k): Diurnal variations in % differences between the mean N_mF_2 values recorded during the March equinox and September equinox for the HSA years of 2000, 2001, and 2002, MSA years of 1998, 1999, 2003, 2004, and 2005, and LSA years of 2006, 2007, and 2008 (solar cycle 23 at Grahamstown, South Africa).

Winter anomalies in middle latitude regions have been previously reported [5, 10, 14, 20, 23, 24, 30, 31]. The occurrence of this anomaly has been attributed to the effects of neutral wind composition, temperature, electric field, and other chemical parameters, such as the O/N_2 ratio. Neutral particles are transported from the southern hemisphere to the northern hemisphere during different solar activity epochs [16, 20, 32-39]. Winter anomaly is usually an equatorial and low-latitude ionospheric phenomenon.

3.3 Seasonal and Annual Variations in N_mF_2

Figure 3 shows the seasonal and annual variations in N_mF_2 and the sunspot number corresponding to solar cycle 23 (1998–2008). The data have been grouped into LSA, MSA, and HSA categories. Regular seasonal and annual variations in N_mF_2 (with the sunspot number) are observed. Exceptions were recorded during the June solstice of the MSA year 1999) and HSA years 2000 and

2001. The reverse trend was observed in these cases, i.e., an increase in the sunspot number results in a decrease in N_mF_2. A non-linear relationship was recorded in this case.

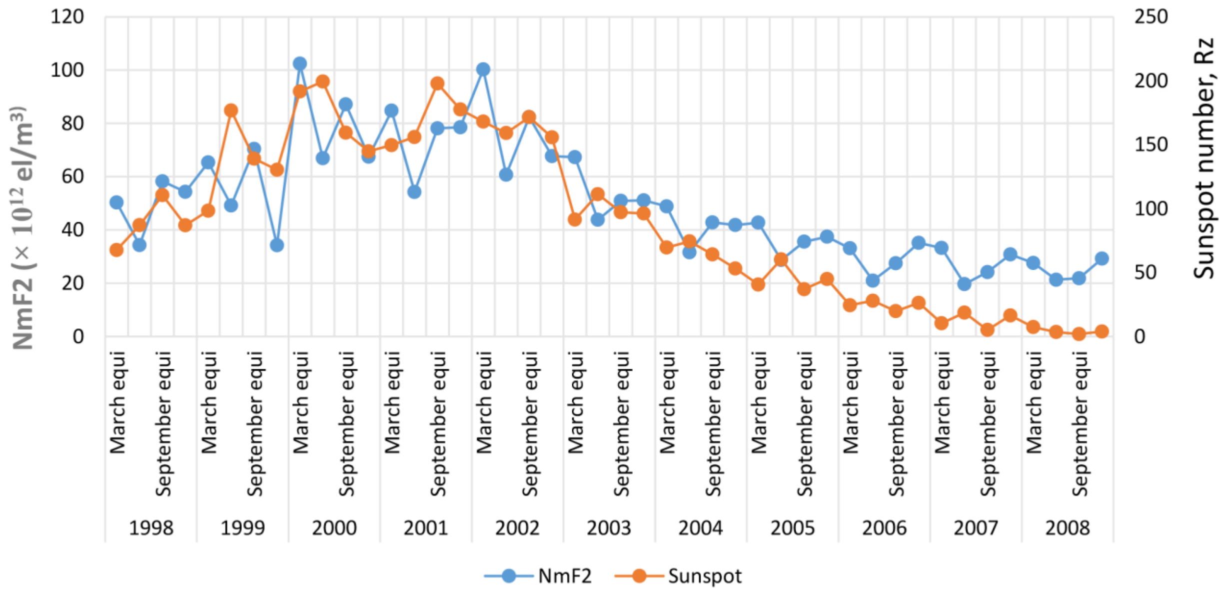

Figure 3 Seasonal and annual variations in N_mF_2 and Sunspot number for the complete solar cycle 23 (1998–2008).

The increase in the sunspot number, Rz, with a decrease in the N_mF_2 is known as the saturation effect. The electron density structure associated with the saturation effect was reported by Balan et al. [40], Balan et al. [41], Sethi et al. [14], and Ogwala et al. [42]. They attributed the origin of this phenomenon to some unknown factors near the earth's environment. The strength of the saturation effect weakens in the middle latitude regions, and it becomes weaker than the saturation effect observed in the equatorial and low latitude regions [43]. The saturation effects observed by us during MSA and HSA were of equal strength.

3.4 Correlation between N_mF_2 and the Sunspot Number, Rz

Figure 4 presents the correlation between the monthly averaged N_mF_2 values and monthly averaged sunspot number for the solar cycle 23 (1998–2008). The results reveal positive and negative correlations, which were generally weak for all the years in the solar cycle considered. An exception was recorded for the MSA year 2005 when an average negative correlation (0.64) was observed. The electron density in the ionosphere is directly proportional to the sunspot number, which is a measure of the degree of the Sun-activity. However, the reason behind the average negative correlation recorded in the MSA year of 2005 could not be established. The negative correlation could potentially be a result of the influence of O/N_2 composition, neutral wind effects, etc. A positive correlation indicates that the N_mF_2 value increases with an increase in the sunspot number [18, 31, 43, 44], and a negative correlation presents the opposite case. Annual, solar cycle and latitudinal variations are observed for the correlation coefficients. These variations are insignificant, and it indicates that other factors influence the N_mF_2 values.

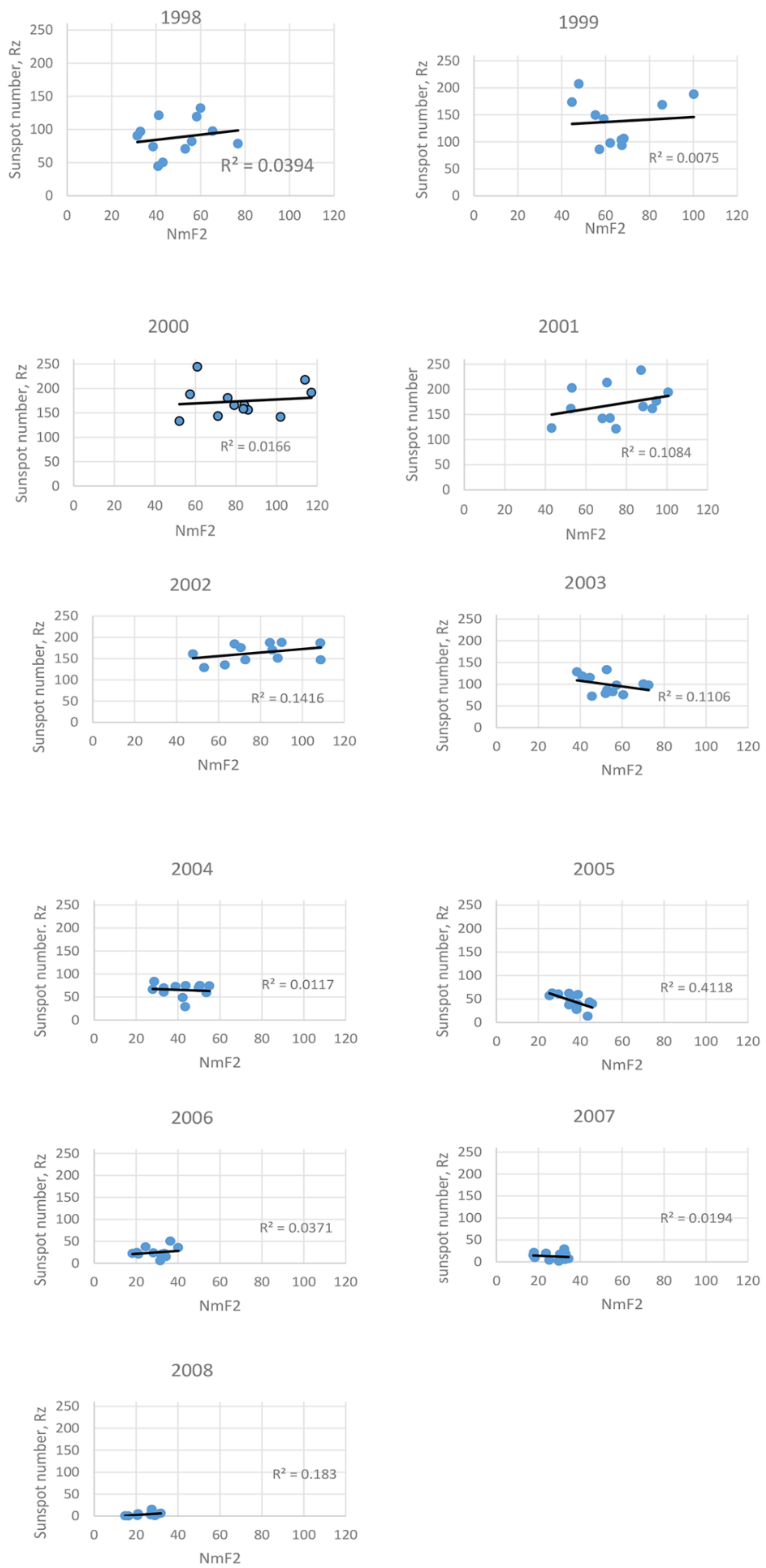

Figure 4 Correlation between N_mF_2 and the sunspot number for solar cycle 23 (1998–2008). The data are classified into the categories of LSA, MSA, and HSA.

It has been previously reported that the correlation coefficient increases with solar activity [43, 45]. However, we did not observe this trend. The average correlation was recorded during the MSA year of 2005 (-0.64), a low correlation was observed during the HSA years of 2001 (0.33) and 2002 (0.38), MSA year of 2003 (-0.33), and LSA year of 2008 (0.43). A negligible correlation was observed for all other years. However, the correlation coefficient did not follow a set trend during the three solar cycle epochs studied by us. This may be attributed to the ionospheric electrodynamic property of the middle latitude regions and the electron density (at the top and bottom of the system) that diffuses toward middle latitude regions.

4. Discussion

Significant solar cycle variations are observed in the middle latitude ionosphere. This can be attributed to the variations in sunspot number observed over 11 years, extreme Ultra-Violet radiations (EUV), and other solar proxies [7, 41, 43]. These phenomena occur despite the fact that it is strategically located between the equatorial/low latitude and polar regions. Although the middle latitude ionospheric regions have been widely studied, the ionospheric variations in the African middle latitude ionospheric region have not been explored. Normally, the N_mF_2 values recorded during the daytime were higher than the N_mF_2 values recorded during the night. This result agrees well with previously reported results [11, 46-49]. However, the seasonal variations in the N_mF_2 values at the middle latitude regions deviate partially or completely from previously reported results. Ayub et al. [16] and Onori et al. [49] reported that the f_oF_2/N_mF_2 values recorded during winter were higher than those recorded during summer (i.e., winter anomaly was observed). Winter anomaly is an ionospheric phenomenon where the number of electrons produced during the winter season (December solstice) is higher than that produced during the summer season (June solstice; Richards, 2001 [50]). However, this is in contrast with some of our results which can be attributed to the variations in the solar zenith angle and the changes in the position of the Sun. During summer, the earth receives more radiation from the Sun, which ionizes the ionosphere. Our results show deviations from this result during the MSA years spanning 2004–2005 and the HSA year of 2001. Thus, nighttime winter anomaly was observed in these cases. The N_mF_2 values recorded during the daytime in these epochs were equal to those recorded during the solstices of the MSA years spanning 2004–2005 and the HSA year of 2001. These deviations may be attributed to the global circulation of atmospheric wind in the middle latitudes regions during different seasons and solar epochs [7]. However, winter anomaly was seen throughout the day during the MSA year of 1998) and the LSA years spanning 2006–2008. The physical parameters responsible for the onset of winter anomaly are the changes in the thermospheric composition attributable to the dominant upwelling/downwelling of molecular/atom-rich air during summer/winter, respectively [51-53]. The noon bite-out phenomenon was observed in all the years for the solar cycle considered during the June solstice. The only exception was observed in the HSA year of 2002 when the appearance of a dome-shaped peak was observed. Although the noon bite-out phenomenon can be observed in the other three seasons, it is not consistent for all the years. We observed that the noon bite-out phenomenon shows seasonal and solar cycle variations. The noon bite-out phenomenon may occur at any latitudinal region of the ionosphere as long as it is restricted to the bottom-side ionosphere. The noon bite-out phenomenon is basically a result of the fountain effect. It indicates electron depletion, resulting from the $E \times B$ drift of the ion density to the ±20° latitudes [31, 54-57]. The amount of solar radiation emitted during ME and SE is usually equal. However, the amount of radiation received varies (in the middle latitude ionospheric region) based on the effects of thermospheric neutral wind composition and other ionospheric dynamic processes, which significantly affect the chemical processes occurring in the ionosphere [7, 52]. The equinoctial asymmetry in the N_mF_2 values observed in the middle latitude region revealed that the ME values were usually higher than the SE values. In a few cases, the SE value was higher than the ME value. Furthermore, we observed that when the sunspot number $R_z$was > 150, a significant reduction in the N_mF_2 value was observed, resulting in the saturation effect [14]. Ma et al. [43] reported the seasonal and latitudinal differences of saturation effect between ionospheric N_mF_2 and solar activity indices for the middle and high latitude regions. The N_mF_2 value did not increase with the solar activity (which increased in summer) and reduced drastically during the other three seasons at the middle latitude regions. At high latitudes in the Northern Hemisphere, a moderate trend of non-linear increase in N_mF_2 with solar activity was observed. This was attributed to the thermospheric global circulation of neutral wind, which introduced seasonal, latitudinal, and North–South differences in the correlation coefficients recorded for the correlation between N_mF_2 and the solar activity indices. Almost equal levels of saturation effects were observed during the June solstice for MSA and HSA. Liu et al. [58] and Kakoti et al. [59] suggested that changes in solar EUV, thermospheric neutral wind composition and ion pressure were also important factors that may give rise to the saturation effect during different epochs of the solar cycle. Hence, the reason behind the generation of the saturation effect should be further investigated to understand its effects on satellite launch processes and satellite Radio communication devices. Finally, the low correlation coefficient recorded by us for the interaction between N_mF_2 and the sunspot number does not agree with the results reported by Balan et al. [60], Balan et al. [61], and Sharma et al. [62], who reported a significant correlation between some ionospheric parameters and solar proxies at their different regions. The insignificant level of correlation between N_mF_2 and the sunspot number can be potentially attributed to the unstable global circulation of thermospheric neutral wind, which can potentially affect the background ionization process occurring at middle latitude regions [43].

5. Conclusions

The variations in N_mF_2 at a middle latitude station of Grahamstown, South Africa (solar cycle 23; low, moderate, and high solar activity epochs) were studied. Anomalous equatorial and low latitude ionospheric features for N_mF_2 (such as the noon bite-out phenomenon) were observed. Noon bite-out is not a middle-latitude ionospheric phenomenon. This phenomenon was observed during the June solstice for most of the years during the solar cycle. However, it was not observed during the other three seasons. The seasonal and annual variations present a saturation effect/non-linear relationship between N_mF_2 and the sunspot number during the June solstice of the MSA year 1999 and the HSA years spanning 2000–2001. Weak positive and negative correlation between N_mF_2 and the sunspot number was recorded for most of the years of the solar cycle (exception: the MSA year of 2005; average negative correlation). The insignificant correlation between N_mF_2 and the sunspot number should be investigated further in the future. The results reported herein can potentially help augment the results reported previously on the seasonal variations in N_mF_2 over the middle latitude African sector.

Acknowledgments

Data from the South African Ionosonde network is made available by the South African National Space Agency (SANSA), who we acknowledge for facilitating and coordinating the continued availability of data. We also acknowledge National Geophysical Data Center (NGDC) for providing values of sunspot number.

Author Contributions

O.A was the principal researcher and main author of the manuscript. O.E., S.E. and O.C. supervised the research work. O.A. and A.R.A reviewed the manuscript. O.O. supervised the research, while K.Y., O.O. and O.J. proofread for grammar errors.

Competing Interests

The authors declare that they have no competing interests.

References

1. Ratcliffe JA. An introduction to the ionosphere and magnetosphere. Cambridge: University Press Cambridge; 1972.
2. Akala AO, Oyeyemi EO, Somoye EO, Adeloye AB, Adewale AO. Variability of foF2 in the African equatorial ionosphere. Adv Space Res. 2010; 45: 1311-1314.
3. Richmond AD, Lu G. Upper-atmospheric effects of magnetic storms: A brief tutorials. J Atmos Sol Terr Phys. 2000; 62: 1115-1127.
4. Rishbeth H, Garriot O. Introduction to ionospheric physics. New York: Academic Press; 1969.
5. Lee WK, Kil H, Kwak YS, Wu Q, Cho S, Park JU. The winter anomaly in the middle-latitude F region during the solar minimum period observed by the constellation observing system for meteorology, ionosphere, and climate. J Geophys Res Space Phys. 2011; 116: A02302.
6. Somoye EO. Comparison of N_mF_2 variability at Ibadan, Singapore and Slough during different epochs of solar cycle. Asian J Sci Res. 2009; 2: 155-160.
7. Chen Y, Liu L, Wan W, Ren Z. Equinoctial symmetry in solar activity variations of N_mF_2 and TEC. Ann Geophys. 2012; 30: 613-622.
8. Aggarwal M, Bardhan A, Sharma DK. Equinoctial asymmetry in ionosphere over Indian region during 2006-2013 using COSMIC measurements. Adv Space Res. 2017; 60: 999-1014.
9. Talha M, Ahmed N, Ameen MA, Sapundjiev D, Murtaza G. Equinoctial asymmetry during solar minima at low to middle latitude. Adv Space Res. 2022; 70: 2941-2952.
10. Torr MR, Torr DG. The seasonal behavior of the F2 layer of the ionosphere. J Atmos Terr Phys. 1973; 35: 2237-2251.
11. Torr DG, Torr MR, Richards PG. Causes of F region winter anomaly. Geophys Res Lett. 1980; 7: 301-304.
12. Zou L, Rishbeth H, Muller-Wodard IC, Aylward AD, Millward GH, Fuller-Rowell TJ, et al. Annual and semi-annual variations in the ionospheric F2 layer. I. Modelling. Ann Geophys. 2000; 18: 927-944.
13. Mikhailov AV, Forster M, Leschinskaya TY. On the mechanism of the post-midnight winter N_mF_2 enhancements: Dependence on solar activity. Ann Geophys. 2000; 18: 1422-1434.

14. Sethi NK, Goel MK, Mahajan KK. Solar cycle variations of foF2 from IGY to 1990. Ann Geophys. 2002; 20: 1677-1685.
15. Farelo AF, Herraiz M, Mikhailov AV. Global morphology of night-time N_mF_2 enhancements. Ann Geophys. 2002; 20: 1795-1806.
16. Ayub M, Iqbal S, Ameen MA, Reinisch BW. Study of maximum electron density N_mF_2 at Karachi and Islamabad during solar minimum (1996) and solar maximum (2000) and its comparison with IRI. Adv Space Res. 2009; 43: 1821-1824.
17. Knyazeva MA, Namgaladze AA. Magnetospheric and thermospheric origin electric fields influence on the enhanced electron density regions in the night-time ionospheric F2-layer. Phys Auroral Phenom. 2011; 33: 117-120.
18. Adebesin BO. foF2 variations during geomagnetic disturbances in the rise of solar cycle 23. Indian J Radio Space Phys. 2012; 41: 323-331.
19. Adebesin BO, Adekoya BJ, Ikubanni SO, Adebiyi SJ, Adebesin OA, Joshua BW, et al. Ionospheric foF2 morphology and response of F2 layer height over Jicamarca during different solar epochs and comparison with IRI-2012 model. J Earth Syst Sci. 2014; 123: 751-765.
20. Su F, Wang W, Burni AG, Yue X, Zhu F, Lin J. Statistical behavior of the longitudinal variations of daytime electron density in the topside ionosphere at middle latitude. J Geophys Res Space Phys. 2016; 121: 11560-11573.
21. Adebesin BO, Rabiu AB, Obrou OK, Adeniyi JO. Ionospheric peak electron density and performance evaluation of IRI-CCIR near magnetic equator in Africa during two extreme solar activities. Space Weather. 2018; 16: 230-244.
22. Chou VT, Lee CC. Ionospheric variability at Taiwan low latitude station: Comparison between observation and IRI-2001 model. Adv Space Res. 2008; 42: 673-681.
23. Strobel DF, McElroy MB. The F2 layer at middle latitude. Planet Space Sci. 1970; 18: 1181-1202.
24. Buonsanto MJ. Observed and calculated F2 peak height and derived meridional winds at middle latitudes over a full solar cycle. J Atmos Terr Phys. 1990; 52: 223-240.
25. Gnabahou A, Quattara F. Ionospheric variability from 1957–1981 at Djibouti. Eur J Sci Res. 2012; 73: 382-390.
26. Somoye EO, Akala AO. Comparison of diurnal, seasonal and latitudinal effect of MUF VR and N_mF_2 VR during some solar cycle epochs. Adv Space Res. 2011; 47: 2182-2187.
27. Mukaka MM. Statistics corner: A guide to appropriate use of correlation coefficient in medical research. Malawi Med J. 2012; 24: 69-71.
28. Abadi P, Yuichi O, Takuya T. Effects of pre-reversal enhancement of E × B drift on the latitudinal extension of plasma bubble in Southeast Asia. Earth Planets Space. 2020; 67: 74.
29. Ghosh P, Yuichi O, Sivakandan M, Hiroyuki S. Day-to-day variation of pre-reversal enhancement in the equatorial ionosphere based on GAIA model simulations. Earth Planets Space. 2020; 72: 93.
30. Xu J, Ma R, Wang W. Terannual variations in the F2 layer peak electron density at middle latitudes. J Geophys Res. 2012; 117: A01308.
31. Ogwala A, Somoye EO, Panda SK, Ogunmodimu O, Onori EO, Sharma SK, et al. Total electron content at low-, middle-, and high-latitudes in the African longitude sector and its comparison with IRI-2016 and IRI Plas-2017 models. Adv Space Res. 2021; 68: 2160-2176.
32. Jin SG, Luo OF, Park P. GPS observations of the ionospheric F2-layer behaviour during the 20th November 2003 geomagnetic storm over South Korea. J Geod. 2008; 82: 883-892.

33. Yadav S, Dabas RS, Das RM, Upadhayaya AK, Sharma K, Gwal AK. Diurnal and seasonal variation of F2-layer ionospheric parameters at equatorial ionization anomaly crest region and their comparison with IRI-2001. Adv Space Res. 2009; 45: 361-367.
34. Magdaleno S, Altadill D, Herraiz M, Blanch E, Morena BD. Ionospheric peak height behavior for low, middle and high latitudes: A potential empirical model for quiet conditions—Comparison with the IRI-2007 model. J Atmos Solar Terr Phys. 2011; 73: 1810-1817.
35. Ameen MA, Khursheed H, Jabbar MA, Ali MS, Chishtie F. Variation of hmF2 and N_mF_2 deduced from DPS-4 over Multan (Pakistan) and their comparisons with IRI-2012 and IRI-2016 during the deep solar minimum between cycles 23 and 24. Adv Space Res. 2018; 61: 1726-1735.
36. Rao SS, Chakraborty M, Pandey R. Ionospheric variations over Chinese EIA region using foF2 and comparison with IRI-2016 model. Adv Space Res. 2018; 62: 84-93.
37. Liu Z, Fang H, Wang L, Niu J, Meng X. A comparison of ionosonde measured foF2 and IRI-2016 predictions over China. Adv Space Res. 2019; 63: 1926-1936.
38. Arikan F, Sezen U, Gulyaeva T. Comparison of IRI-2016 F2 layer model parameters with ionosonde measurements. J Phys Res. 2019; 124: 8092-8109.
39. Zhang B, Wang Z, Shen Y, Li W, Xu F, Xiaoxiao L. Evaluation of foF2 and hmF2 parameters to IRI-2016 model in different latitudes over China under high and low solar activity years. Remote Sens. 2022; 14: 860.
40. Balan N, Bailey GJ, Moffett RJ. Modelling studies of ionospheric variations during an intense solar cycle. J Geophys Res. 1994; 99: 17467-17475.
41. Balan N, Bailey GJ, Su YZ. Variations of the ionosphere and related solar fluxes during solar cycle 21 and 22. Adv Space Res. 1996; 18: 11-14.
42. Ogwala A, Somoye EO, Ogunmodimu O, Adeniji-Adele RA, Onori EO, Oyedokun OJ. Diurnal, seasonal and solar cycle variations in total electron content and comparison with IRI-2016 model at Birnin Kebbi. Ann Geophys. 2019; 37: 775-789.
43. Ma R, Xu J, Wang W, Yuan W. Seasonal and latitudinal differences of the saturation effects between ionospheric NmF2 and solar activity indices. J Geophys Res. 2009; 114: A10303.
44. Mielich J, Bremer J. Long-term trends in the ionospheric F2 region with different solar activity indices. Ann Geophys. 2013; 31: 291-303.
45. Liu L, Wan W, Chen Y, Le H. Solar activity effects on the ionosphere: A brief review. Sci Bulletin. 2011; 56: 1202-1211.
46. Richards PG, Torr DG, Reinisch BW, Gamache RR, Wilkinson PJ. F2 peak electron density at Millstone hill and Hobart: Comparison of measurement and theory at solar maximum. J Geophys Res. 1994; 99: 15005-15016.
47. Mikhailov AV, Depueva VH, Depueva AH. Synchronous N_mF_2 and NmE daytime variations as a key to the mechanism of quiet-time F2-layer disturbances. Ann Geophys. 2007; 25: 483-493.
48. Mikhailov AV, Perrone L. On the mechanism of seasonal and solar cycle N_mF_2 variations: A quantitative estimate of the main parameters contribution using incoherent scatter radar observations. J Geophys Res. 2011; 116: A03319.
49. Onori EO, Ometan OO, Adeniji-Adele RA, Ogungbe AS, Ogabi CO, Ogwala A, et al. Seasonal response of peak electron density of F2-layer in the African and American Sectors during low solar activity period of cycle 24. Appl Phys. 2021; 4: 1-10.
50. Richards PG. Seasonal and solar cycle variations of the ionospheric peak electron density: Comparison of measured and models. J Geophys Res. 2001; 106: 12803-12819.

51. Rishbeth H. The equatorial F layer: Progress and puzzles. Ann Geophys. 2000; 18: 730-739.
52. Aggarwal M, Joshi HP, Iyer KN, Kwak YS, Lee JJ, Chandra H, et al. Day-to-day variability of equatorial anomaly in GPS-TEC during low solar activity period. Adv Space Res. 2012; 49: 1709-1720.
53. Ogwala A, Onori EO, Kayode YO, Adeniji-Adele RA, Somoye EO. The Equatorial Ionospheric phenomena: A review of past studies, government interest and unsolved problems. Lat Am J Phys Educ. 2022; 16: 2303-1-2303-9.
54. Rajaram G, Rastogi RG. Equatorial electron density–Seasonal and solar cycle changes. J Atmos Terr Phys. 1977; 39: 1175-1182.
55. Yeh KC, Franke SJ, Andreeva ES, Kunitsyn VE. An investigation of motions of the equatorial anomaly crest. Geophys Res Lett. 2001; 28: 4517-4520.
56. Lee CC. Examination of the absence of noontime bite-out in equatorial total electron content. J Geophys Res Space Phys. 2012; 117: A09303.
57. Eyelade VA, Adewale AO, Akala AO, Bolaji OS, Rabiu AB. Studying the variability in the diurnal and seasonal variations in GPS total electron content over Nigeria. Ann Geophys. 2017; 35: 701-710.
58. Liu L, Wan W, Ning B, Pirog OM, Kurkin VI. Solar activity variations of the ionospheric peak electron density. J Geophys Res. 2006; 111: A08304.
59. Kakoti G, Bhuyan PK, Hazarika R. Seasonal and solar cycle effects on TEC at 95°E in the ascending half (2009–2014) of the subdued solar cycle 24: Consistent underestimation by IRI-2012. Adv Space Res. 2017; 60: 257-275.
60. Balan N, Bailey GJ, Jayachandran B. Ionospheric evidence for a nonlinear relationship between the solar EUV and 10.7 cm fluxes during an intense solar cycle. Planet Space Sci. 1993; 41: 141-145.
61. Balan N, Bailey GJ, Jenkins B, Rao PB, Moffet J. Variations of ionospheric ionization and related solar fluxes during an intense solar cycle. J Geophys Res. 1994; 99: 2243-2253.
62. Sharma SK, Singh AK, Panda SK, Ansari K. GPS derived ionospheric TEC variability with different solar indices over Saudi Arabia. Acta Astronaut. 2020; 174: 320-333.